Lidar observations revealing transport of O_3 in the presence of a nocturnal low-level jet: Regional implications for "next-day" pollution

John T. Sullivan [a,*], Scott D. Rabenhorst [b], Joel Dreessen [c], Thomas J. McGee [a], Ruben Delgado [d], Laurence Twigg [e], Grant Sumnicht [e]

[a] NASA Goddard Space Flight Center, Chemistry and Dynamics Laboratory, Greenbelt, MD 20771, USA
[b] National Research Council/Naval Research Laboratory, Washington DC 20375, USA
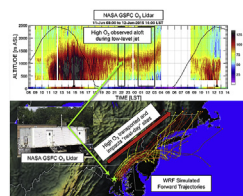[c] Maryland Department of the Environment, Air Monitoring Program, Baltimore, MD 21230, USA
[d] Joint Center for Earth Systems Technology, Baltimore, MD 21250, USA
[e] Science Systems and Applications Inc., Lanham, MD 20706, USA

HIGHLIGHTS

- First O_3 lidar profiles during a nocturnal low-level jet in Mid-Atlantic U.S.
- Observations confirm residual layer pollutants mixing down during onset of jet.
- Nocturnal turbulent mixing impacted surface O_3 and its precursors.
- Model simulations indicate regional transport and boundary layer entrainment of O_3.
- Surface monitors confirm jet transport can impact the "next-day" chemical budget.

GRAPHICAL ABSTRACT

ABSTRACT

Remotely sensed profiles of ozone (O_3) and wind are presented continuously for the first time during a nocturnal low-level jet (NLLJ) event occurring after a severe O_3 episode in the Baltimore-Washington D.C. (BW) urban corridor throughout 11–12 June 2015. High-resolution O_3 lidar observations indicate a well-mixed and polluted daytime O_3 reservoir, which decayed into a contaminated nocturnal residual layer (RL) with concentrations between 70 and 100 ppbv near 1 km above the surface. Observations indicate the onset of the NLLJ was responsible for transporting polluted O_3 away from the region, while simultaneously affecting the height and location of the nocturnal residual layer. High-resolution modeling analyses and next-day (12 June) lidar, surface, and balloon-borne observations indicate the trajectory of the NLLJ and polluted residual layer corresponds with "next-day" high O_3 at sites throughout the southern New England region (New York, Connecticut, Massachusetts). The novel O_3 lidar observations are evidence of both nocturnal advection (via high NLLJ wind fields) and entrainment of the polluted residual layer in the presence of the "next-day" convectively growing boundary layer. In the greater context, the novel observational suite described in this work has shown that the chemical budget in areas downwind of major urban centers can be altered significantly overnight during transport events such as the NLLJ.

* Corresponding author.
 E-mail address: john.t.sullivan@nasa.gov (J.T. Sullivan).

1. Introduction

Vertical mixing associated with buoyant eddies generally weakens near sunset, which allows stratification within the lowest layers of the atmosphere and the formation of the nocturnal boundary layer (NBL). The NBL usually consists of a stable surface layer (SL), which develops near the surface through radiational cooling resulting in an inversion layer, and a residual layer (RL), which extends from the top of the SL inversion upwards to the daytime mixing height [Stull, 1988; Klein et al., 2014]. During nighttime stratification of the atmosphere, pollutants (such as ozone (O_3)) that were well mixed during the daytime begin to heterogeneously separate into the SL and RL between the inversion(s) [Zhang and Rao (1999); Tong et al., 2011]. Throughout the nighttime SL, O_3 is depleted due to dry deposition, suppressed vertical mixing and titration from nitric oxide (NO) to form nitrogen dioxide (NO_2) [Trainer et al., 1993; Jacob, 2000]. Nighttime increases in surface O_3 in the Baltimore-Washington D.C. (BW) region are known to occur; one mechanism that has been identified as a source is the nocturnal low-level jet (NLLJ) mixing RL pollutants towards the surface [Corsmeier et al., 1997; Ryan, 2004; Hu et al., 2012; Delgado et al., 2014; Rabenhorst et al., 2014]. However, continuous profiles of O_3 are necessary to understand the horizontal extent and "next-day" implications of the RL and nocturnal surface increases.

Typical NLLJs in the Mid-Atlantic (MA) United States occur in the presence of light synoptic winds, where orographic induced temperature gradients drive a layer of fast moving air that is frictionally decoupled from the surface due to a sudden decrease in buoyant eddy viscosity [Beyrich 1994; Ryan et al., 1998; Ryan 2004; Delgado et al., 2014; Rabenhorst et al., 2014]. The sloping MA topography, with the Appalachian Mountains to the west and the Atlantic Ocean to the east, typically produces a NLLJ with southwesterly flow [Zhang et al., 2006] that can be enhanced ahead of approaching cold fronts [Rabenhorst et al., 2014].

It is hypothesized from surface and balloon-borne observations that increases in O_3 associated with the NLLJ originates from a combination of regional advection and turbulent vertical mixing [Corsmeier et al., 1997; Ryan 2004; Seaman and Michelson, 2000, Hu et al., 2012, 2013]. Moreover, the high wind speeds at the NLLJ core are responsible for 1) transporting air pollutants over hundreds of kilometers (and multiple state lines) during night time and 2) turbulently mixing pollutants (via vertical wind shear) above and below the higher wind speeds within the jet core [Corsmeier et al., 1997; Seaman and Michelson, 2000; Poulos et al., 2002; Taubman et al., 2004; Banta et al., 2007; Delgado et al., 2014; Rabenhorst et al., 2014].

Although the framework for the meteorological conditions of NLLJ formation in the MA region have been well documented [Rabenhorst et al., 2014], the vertical and horizontal effects on O_3 transport during NLLJ conditions are less detailed. A common metric for typifying whether a NLLJ is "transport relevant" is to determine the duration (e.g. >5 h) of the jet [Ryan 2004]. However without continuous profiles of O_3 it is impossible to assess the vertical locations and concentrations of ozone aloft or throughout the RL; this is the necessary information to accurately determine whether a NLLJ is "transport relevant".

Balloon-borne O_3 and wind profiles under NLLJ conditions are scarce, but previous work in the MA has shown that downward transport and entrainment of polluted RL species has contributed to increased concentrations and more efficient production of O_3 throughout the day [Zhang and Rao 1999; Yorks et al., 2009; Hu et al., 2012; Delgado et al., 2014]. On the contrary, modeling analyses from Hu et al., 2013 have shown a marked decrease in "next

day" surface O_3, as a result of more efficient removal via chemical reactions and dry deposition. However, with isolated and infrequent sonde launches, it is difficult to characterize a complete temporal history of potential NLLJ-induced changes such as the extent of vertical mixing/entrainment, RL location [Morris et al., 2010], and transport impacting "next-day" chemical concentrations. Furthermore, it is problematic for model simulations to accurately reproduce the NBL depth and vertical mixing of O_3 within, particularly in the presence of a NLLJ [Zhang and Rao 1999; Aneja et al., 2000; Zhang et al., 2001; Salmond and McKendry 2002; Hu et al., 2012]; although sensitivity analyses have shown to improve the accuracy of simulations [Hu et al., 2013]. Thus accurate and continuous vertical profile information regarding winds and O_3 concentration throughout the RL is critical for correctly simulating transport during the NLLJ and surface impacts. Therefore, to accurately characterize urban pollution events as well as turbulent nocturnal events it is important to co-locate continuous measurements of the vertical profiles of O_3 and wind [McKendry et al., 1997; Banta et al., 1998; Ancellet and Ravetta, 2005; Drobinski et al., 2007; Tucker et al., 2010; Kuang et al., 2011]. For this reason, the National Aeronautics and Space Administration Goddard Space Flight Center Tropospheric O_3 Differential Absorption Lidar (NASA GSFC TROPOZ DIAL) [Sullivan et al., 2014] was deployed to Beltsville, MD during Summer 2015 to augment a radar wind profiler and a broad suite of other co-located atmospheric monitors currently operated by the Maryland Department of the Environment (MDE) [MDE, 2015].

With the suite of co-located instruments, remotely sensed profiles of O_3 and wind are presented for the first time during a NLLJ event occurring after a severe O_3 episode in the BW region on 11–12 June 2015. In section 2, we present surface observations assessed initially at the policy relevant averaging time of 1 and 8 h (section 2.1), followed by chemical and meteorological analyses at 1-min resolution (section 2.2). In section 3, we present a nearly 30-h time-series of O_3 lidar and radar wind observations, which indicate the well-mixed and polluted daytime O_3 reservoir decaying into a polluted nocturnal RL, which persisted into the subsequent morning. To further understand the regional context of these observations and the evolution of RL air mass, meteorological simulations (section 4.1) and next day surface observations (section 4.2) are utilized to characterize the NLLJ-transported/entrained air mass from the BW urban corridor to several states within the southern New England region (New York, Connecticut, Massachusetts). We then summarize our findings in section 5 and place the importance of the results in the context of tightening regulatory standards.

2. Ground level observations in Maryland

2.1. Policy relevant ozone monitoring

During the daytime hours on 11 June 2015, six rural/suburban sites throughout Maryland observed maximum daily 8-h average (MDA8) O_3 concentrations that violated the 75 ppbv 2008 National Ambient Air Quality Standards (NAAQS) (Fig. 1). The pre-established MDE regulatory sites that were in exceedance were Aldino, Fair Hill, Padonia, Rockville, Beltsville, and Howard University (HU)-Beltsville; four additional sites would have exceeded the revised 2015 70 ppbv NAAQS [EPA, 2015] (Edgewood, Essex, Millington, and South Carroll). Observations, and their policy relevance, supporting the photochemical and meteorological mechanisms that caused these sites to exceed the O_3 NAAQS are presented in Dreessen et al. (2016), which describes Canadian wildfire smoke impacting regional air quality. The current work aims to extend the analyses presented in Dreessen et al. (2016) to
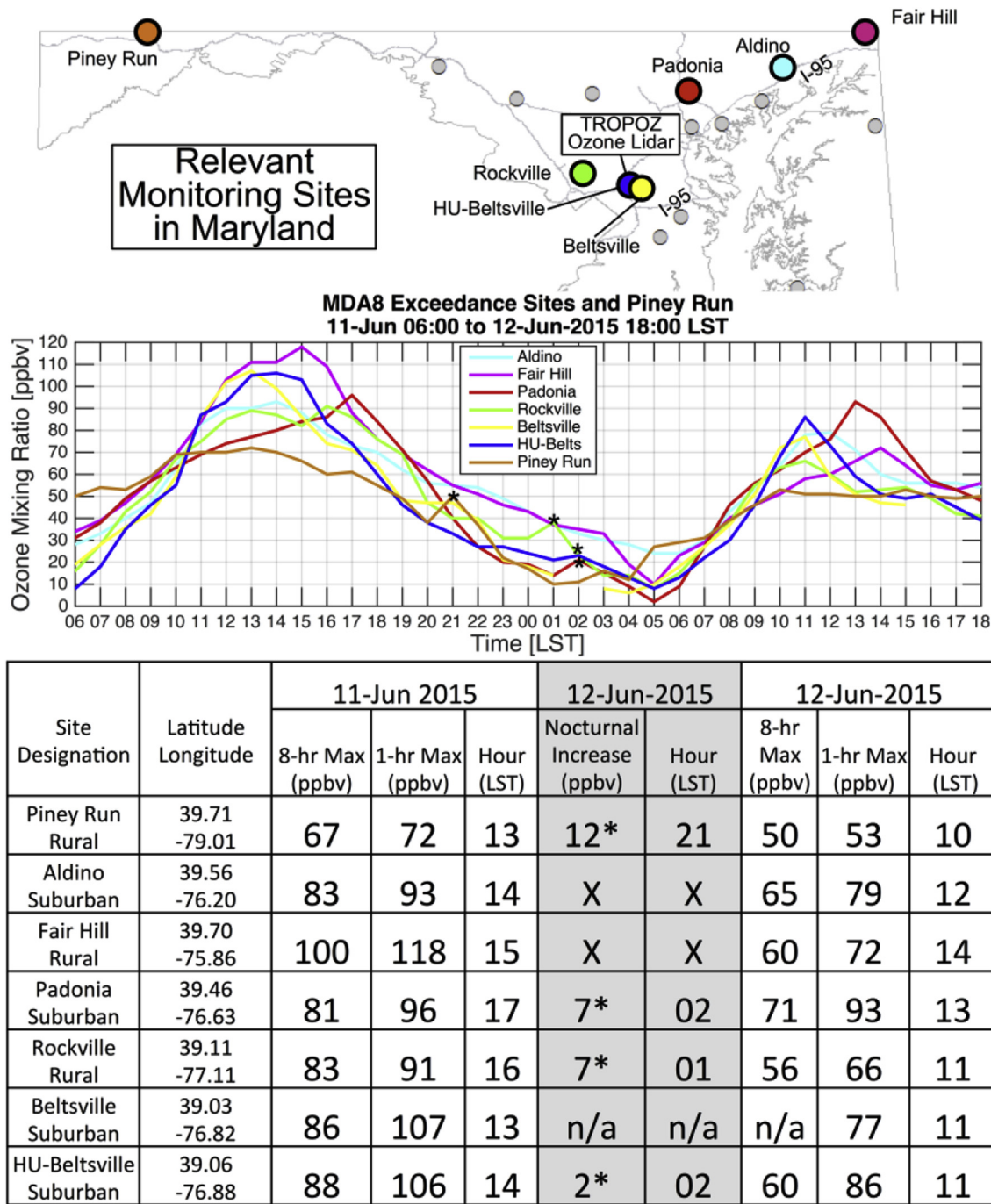
Fig. 1. (Top) Map of relevant Maryland monitoring sites for this case study. (Middle) Time series of O_3 concentrations from 11 to 12 June 2015 for sites within MD that violated the MDA8 standard on 11 June 2015. Piney Run is also shown as a higher altitude (766 m ASL) site. (Bottom) O_3 concentrations presented as 8-hr averages (MDA8), 1-hr averages, and the time of the peak 1-hr concentrations for the daytime and nighttime values on 11–12 June 2015. Nocturnal increases in O_3 are denoted with asterisks to indicate the increases (besides Piney Run) occurred with 1-hr of each other. Intermittent data at the Beltsville monitor on 12 June is the cause of the n/a status. Data provided by the EPA AIRNOW [http://www.airnowtech.org/data].

the lesser-characterized night-time transport and vertical mixing/entrainment of O_3 in the context of "next-day" O_3 exceedances.

The Piney Run monitor (Fig. 1) at an elevation of approximately 766 m above sea level (ASL) is useful for monitoring aloft concentrations of O_3 directly within the RL. This monitor sampled an increase in hourly surface O_3 concentrations of 12 ppbv (denoted with asterisk) during nighttime hours between 21:00 and 22:00 LST on 11 June 2015. Additionally, three sites (Padonia, Rockville,

HU-Beltsville) observed non-negligible (2–7 ppbv, denoted with asterisks) increases in hourly concentrations during nighttime between 01:00 and 03:00 LST. With the absence of photochemical production of O_3 during the night, these surface increases are attributed to a combination of nocturnal advection and vertical mixing between the RL and SL.

Sites (besides Piney Run) in Fig. 1 that received a nocturnal contribution of O_3 (Padonia, Rockville, HU-Beltsville) had an

average 1-hr daily max of 6 ppbv (81.5 vs. 75.5 ppbv) higher peak hourly concentrations on June 12 than sites that did not exhibit a nocturnal increase. Although only small fractions of the polluted nocturnal RL reached the SL during the night, these higher "next-day" peak O_3 values imply the sites were poised for more severe impacts of RL entrainment within the growing planetary boundary layer (PBL) on the following morning [Zhang and Rao, 1999; Talbot et al., 2005; Hu et al., 2012, 2013]. With the strengthening of the current regulatory standards, this early morning "next-day" RL entrainment process could potentially put a regulatory site above the updated MDA8 NAAQS limits for the BW region. For example, the Padonia monitor experienced a nocturnal increase of 7 ppbv and went on to exceed the updated 2015 MDA8 NAAQS on June 12.

2.2. High-resolution surface observations from MDE at Beltsville, MD

To further characterize the air mass observed by the ozone lidar and radar wind profiler at the HU-Beltsville site, Fig. 2 presents surface measurements of a) O_3 and particulate matter less than 2.5 μm (PM 2.5), b) NO, NO_2, and other nitrogen reservoir species (NO_y), c) temperature and relative humidity (RH), and d) wind speed and direction. With the higher resolution surface data, the nocturnal gradients observed in Fig. 1 are more pronounced and two active temporal segments have been isolated to denote variations in the air mass. Segment 1 occurs on 11 June 2015 from 21:30 and 22:30 LST and segment 2 occurs on 12 June 2015 from 00:30 to 03:00 LST. Although these observations are largely used to track discrete times of NLLJ air mass reaching the surface, they are important in understanding the chemical composition of the nocturnal RL and its potential impacts on "next day" O_3 production.

The 1-min observations (Fig. 2a) indicate O_3 increased by nearly 16 ppbv and an additional 10–12 ppbv increase during segment 2. Hourly observations of PM 2.5 denote a value of 26 μgm^{-3} during segment 1 and values reach 29 μgm^{-3} by the end of segment 2. Notably, the hourly PM 2.5 concentrations in segment 2 recorded the peak 1-hr concentrations at the HU-Beltsville monitor for 12 June 2015 and is described further in Dreessen et al. (2016). During night, increases in O_3 are not attributed to direct photochemical mechanisms; however observations of the oxides of nitrogen (Fig. 2b) are used to quantify changes in the chemical budget for O_3 photochemistry in the post-NLLJ condition (Hu et al., 2012, 2013). Throughout the nighttime observations, NO_2

Increases near a maximum near segment 1. There is a pronounced peak of NO_y (NO + NO_2 + all nitrogen reservoir species such as nitric acid peroxyacetyl nitrate (PAN), and nitrous acid) during segment 1. For the month of June 2015, nighttime concentrations of NO_2 and NO_y at the HU-Beltsville, MD site were mostly between 3 and 5 ppbv [www.airnowtech.org/data], indicating segment 1 and 2 had concentrations 2–3 times higher than ambient conditions. Analyses presented in Dreessen et al. (2016) suggest increasing concentrations of PAN, a complex O_3 precursor associated with wildfire transport [Jaffe and Wigder, 2012] being responsible for the difference in NO_x and NO_y during this segment. Segment 2 shows mostly persistent conditions of NO_2 and NO_y from 5 to 7 ppbv. By 06:00 LST, locally produced O_3 precursors associated with early morning mobile emissions become the dominant source of nitrogen oxides [Zhang and Rao 1999; Yorks et al., 2009; Hu et al., 2013; Delgado et al., 2014].

Observations of temperature and RH (Fig. 2c) demonstrate the nocturnal increases in O_3 during segment 1 and 2 were associated with warmer air (increases from 25.5 to 27.2 °C and 21.6–24.4 °C, respectively). Decreases in RH as compared to ambient conditions during these segments also occur. The Sterling, VA radiosonde launches on 11 June 2015 at 19:00 LST and 12 June 07:00 LST (Fig. 3,

http://weather.uwyo.edu/upperair/sounding.html) indicate a RL top height near 1700 m ASL and 2 200 m ASL, respectively as determined by water vapor mixing ratios (Fig. 3a) and equivalent potential temperatures (Fig. 3b). These soundings both show a well-mixed RL and the 19:00 LST launch sampled an environmental lapse rate between 8.9 and 9.5 °Ckm^{-1} within the first 1 000 m. Assuming the polluted air masses were brought down adiabatically to penetrate the SL, the environmental lapse rate indicates the surface air mass descended from an origin height within the RL of 180–190 and 295–315 m AGL, respectively.

The wind speeds (Fig. 2d) nearly tripled during segment 1 and 2 and were mainly associated with strong southerly winds near 1.5 ms^{-1}. Both segments were followed by mostly light (<0.5 ms^{-1}) easterly flow. These abrupt increases in southerly surface wind speeds are an indication of the onset of a NLLJ [Rabenhorst et al., 2014]. Thus, the combination of gradients in chemical and meteorological parameters implies the presence of a polluted air mass that originated in the RL and impacted the SL overnight. Because of the increase in the aerosol, nitrogen species (including PAN), and O_3 content, these measurements confirm the RL significantly affected the nocturnal chemical reservoir and impacted the following morning's chemical budget.

3. Ozone lidar and wind profiler observations in Maryland

3.1. Characterizing the high-O_3 event, residual layer, and low-level jet

Although surface sampling is useful, the critical measurement needed to fully understand NLLJ dynamics and its impacts on transport of O_3 (e.g. the depth and pollution levels of the RL, "next-day" morning entrainment) are continuous vertical profiles of O_3 before, during, and after the NLLJ event. For these reasons, vertical measurements of tropospheric O_3 (Fig. 4a) within the polluted conditions at the HU-Beltsville site were collected with the GSFC TROPOZ DIAL [Sullivan et al., 2014]. The TROPOZ system, a charter NASA instrument in the Tropospheric Ozone Lidar Network (TOL-Net, http://www-air.larc.nasa.gov/missions/TOLNet/), derives O_3 concentrations to mostly within 10–15% as compared to nearby O_3-sonde profiles [Sullivan et al., 2015a] and has been previously utilized to characterize O_3 episodes such as stratospheric-tropospheric exchange [Sullivan et al., 2015b] and terrain driven recirculation events [Sullivan et al., 2016]. Two O_3-sondes, which were conditioned and prepared with current community standard practices [Thompson et al., 2007], were launched on 11 June 2015 at 14:50 LST and on 12 June 2015 near 12:25 LST and are overlaid on the time series (denoted with black triangle) and the profiles shown in Fig. 5. The 1-min O_3 concentrations from the HU-Beltsville surface monitor (Fig. 2) are shown in the bottom panel of the TROPOZ time series. The MDE radar (915 MHz) wind profiler (Fig. 4b–d) located at the HU-Beltsville site has measured nearly continuous profiles of horizontal and vertical wind speeds and direction since June 2005 [https://madis-data.noaa.gov/cap/profiler] and has been utilized in several previous studies [Compton et al., 2013; Rabenhorst et al., 2014; Delgado et al., 2014] to assess boundary layer processes. The normalized solar radiation.

(Source: Lufft WS510 UMB with silicon-pyranometer) measurement made at the site is also overlaid in each panel of the figure to illustrate the transitions between daytime and nighttime. Segment 1 (11 June 2015 from 21:30 to 22:30 LST) and 2 (12 June 2015 from 00:30 to 03:00 LST), based on observations of chemical and meteorological surface impacts in section 2 are also overlaid on the figure.

A thin layer of high O_3 is observed near the top of the RL in the morning hours of June 11. By 14:00 LST, deep convective mixing has
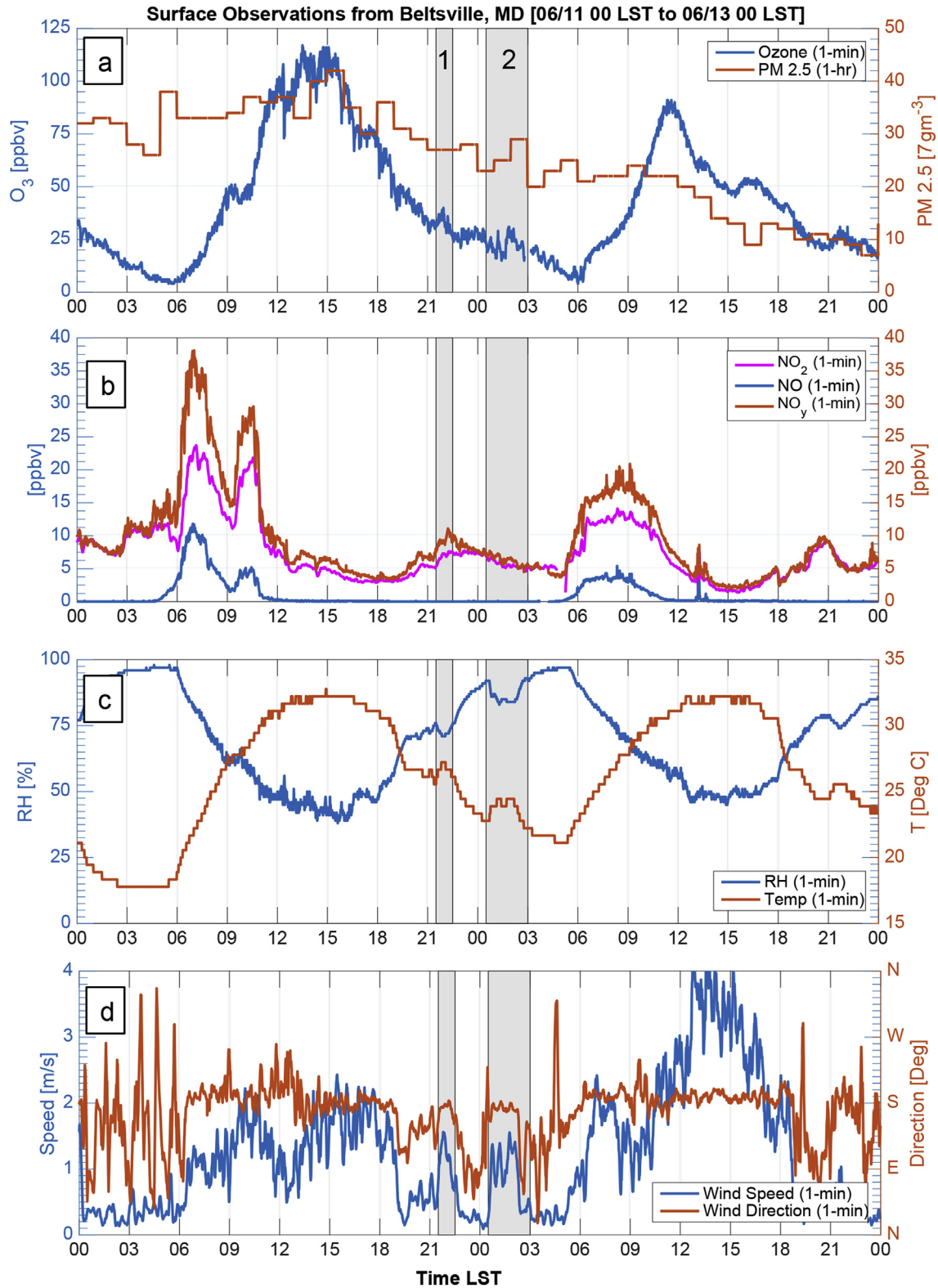
Fig. 2. Time series of a) O_3 and PM 2.5, b) NO, NO_2 and NOy, c) relative humidity and temperature, and d) wind speed and direction from 11 to 12 June 2015 for the HU-Beltsville site. The grey boxes indicate the two time segments where changes in chemical and meteorological parameters were observed during nighttime hours. Each parameter is reported at its highest temporal frequency of 1-min, with the exception of the PM 2.5 monitor at 1-hr. [Source: MDE].
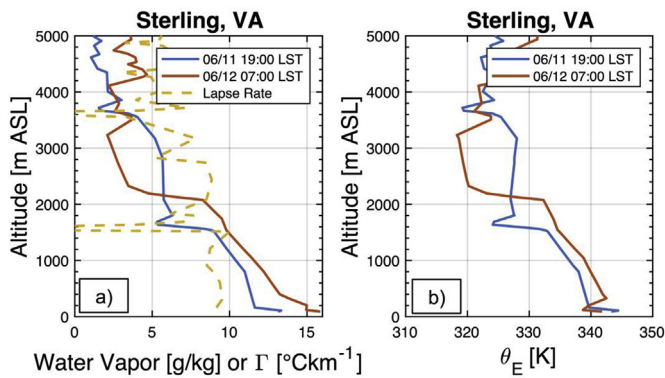
Fig. 3. Water vapor mixing ratio (a) and equivalent potential temperature (b) soundings from Sterling, VA at 19:00 LST on 11 June 2015 and the following on 12 June 2015 at 07:00 LST. The environmental lapse rate from the 19:00 LST sounding is overlaid in panel a [Source: http://weather.uwyo.edu/upperair/sounding.html].

been established within the PBL, likely entraining remaining RL pollutants (including O_3 and precursors). The peak O_3 conditions within the PBL correspond to weak southerly and southwesterly winds between 1 and 2 ms^{-1} (Fig. 4b), indicating the combination of convective mixing in the early morning in the presence of local O_3 precursor emissions under regionally stagnant conditions fueled rapid O_3 production. In this wind regime, the HU-Beltsville site (and all others that exceeded the NAAQS in MD) was situated downwind of the Washington D.C. metro area (including a major interstate beltway, c.f. Top panel in Fig. 1), implying urban emissions idled near the site under quiescent conditions to aid in O_3 formation.

Until 18:00 LST on 11 June, TROPOZ observes O_3 concentrations between 100 and 130 ppbv throughout the PBL to a mixing height between 1700 and 2000 m ASL, forming a 20−30 ppbv gradient between the top of the PBL and the free troposphere. The O_3-sonde launched near 14:50 LST (Fig. 5a), resolves O_3 concentrations mostly between 110 and 120 ppb from the surface to a boundary layer mixing height of 1700 m ASL as determined by the potential temperature (Fig. 5c) and relative humidity (Fig. 5d) profiles. Fig. 5a indicates the lidar and sounding compare well and confirms the use of the O_3 mixing height as a proxy for the PBL height for further analyses.

During the reduction in solar radiation from 18:00 LST until 21:00 LST, TROPOZ observations indicate the daytime polluted convective boundary layer decays into a RL.

With O_3 concentrations between 70 and 100 ppbv from above the surface to 1 500−1700 m ASL. During this diurnal transition, surface concentrations are 20−40 ppbv less than those sampled aloft due to deposition and removal of O_3 via NO$_x$ titration, signifying vertical profiles of O_3 are critical in quantifying RL concentrations and heights. Although O_3 (and water vapor based on the sounding in Fig. 3a) continues to be mostly well mixed, the onset of increased wind speeds increases the vertical stratification of the atmosphere. Within the first 1 000 m of segment 1, wind speeds peak above 14 m s^{-1} (Fig. 4b), wind directions shift to mostly westerly (Fig. 4c), and O_3 concentrations dramatically decline with the onset of a NLLJ [Banta et al., 1998; Ryan 2004].

3.2. Characterizing the nocturnal O_3 increases

Although it was not a policy relevant amount of O_3 that reached the surface overnight, it is important to offer a physical explanation of the processes that occurred as increased concentrations of O_3 precursors (Fig. 2) were also brought to the surface. A surface

increase in O_3 occurs in segment 1 and coincides a few hours after the onset of the NLLJ, indicating the O_3 was mixed down via mechanical turbulence that was strong enough to penetrate the surface inversion layer [Banta et al., 2003]. Vertical eddies and downward drafts, resulting from advection into the BW region, quickly forced polluted RL air under the jet core towards the surface (akin to the "leaky" RL from work shown in Talbot et al., 2005). The onset of a second wind speed maximum occurs near Segment 2. This is associated with 1) another increase of O_3 at the surface and 2) the increase in height of the top of the RL. The increase in O_3 is attributed to the same physical processes occurring in segment 1, downdrafts force polluted air near the middle of the RL towards the surface. The increase in the RL top is associated with a "wedging" affect described in Rabenhorst et al., 2014 in which the advecting NLLJ displaces an air mass vertically upward. Overall, the wind speeds indicate the NLLJ was first observed at the HU-Beltsville site near 20:00 LST and persisted for 10 h (a "transport relevant" duration) until 06:00 LST the following morning.

3.3. Characterizing the "next-day" O_3 profiles

To further illustrate the NLLJ-induced increases of O_3 during the following morning, Fig. 6 shows O_3 concentrations (Fig. 6a) and vertical wind speeds (Fig. 6b) at cascading levels in the atmosphere near 1275, 500, and 350 m ASL from 11 June 16:00 LST to 12 June 08:00 LST. Segment 1 and 2 are both denoted here as have been defined previously, but now a dashed line has been added to identify the peak O_3 concentration in each segment. During segment 1 (and in particular at the dashed line), the 350 and 500 m levels are well-mixed in O_3 concentration (near 70 ppbv, Fig. 6a) and are associated with strong downward velocities (Fig. 6b). Between segment 1 and segment 2 the O_3 concentrations at the 350, 500, and 1 275 m levels begin to decouple while surface concentrations remain unchanged, which is in indication of a return to a stably stratified regime. However during segment 2, the 350 and 500 m O_3 concentrations are very similar, indicating a return to a well mixed regime and are again associated with strong downward velocities (Fig. 6b). The 1 275 m layer during the beginning of segment 2 experiences large downward motion with consistently high (above 85 ppbv) O_3 concentrations and transfers more polluted air towards the lower levels of the atmosphere.

Evidence of early morning convective mixing exists in the downward motion observations near 05:00 LST in the 1 275 m layer. Large downwards drafts indicate entrainment and convective mixing of the polluted RL in the early morning hours of 12 June. TROPOZ observations denote a pronounced and polluted RL persisted until 10:00 LST with O_3 concentrations between 75 and 85 ppbv in a region from 500 to 1200 m ASL. Below 500 m ASL TROPOZ observations of 50−60 ppbv correspond well with those sampled with the surface monitor, further indicating convective mixing and entrainment of the polluted RL into PBL has occurred. By 12:00 LST, TROPOZ observes concentrations of O_3 between 80 and 110 ppbv from 300 m ASL to a mixing height near 1 200 m ASL. The O_3 sonde launched near 12:25 LST (Fig. 5b) indicates an O_3 profile mostly near 85 ppbv and increasing to 100 ppbv up to a PBL height of 1 100 m (based on the potential temperature gradient and RH, Fig. 5c−d). Near 14:00 LST, the winds increase to 8-10 ms^{-1} (28−36 kmhr^{-1}) in a south/southwesterly flow below 1 500 m ASL and ventilate O_3 from towards sites to the northeast. Notably, the Padonia and Aldino sites (situated downwind during this flow pattern in the presence of additional polluted RL precursors) recorded the two highest MDA8 values (and Padonia violated the 2015 NAAQS) for all of Maryland on 12 June 2015.
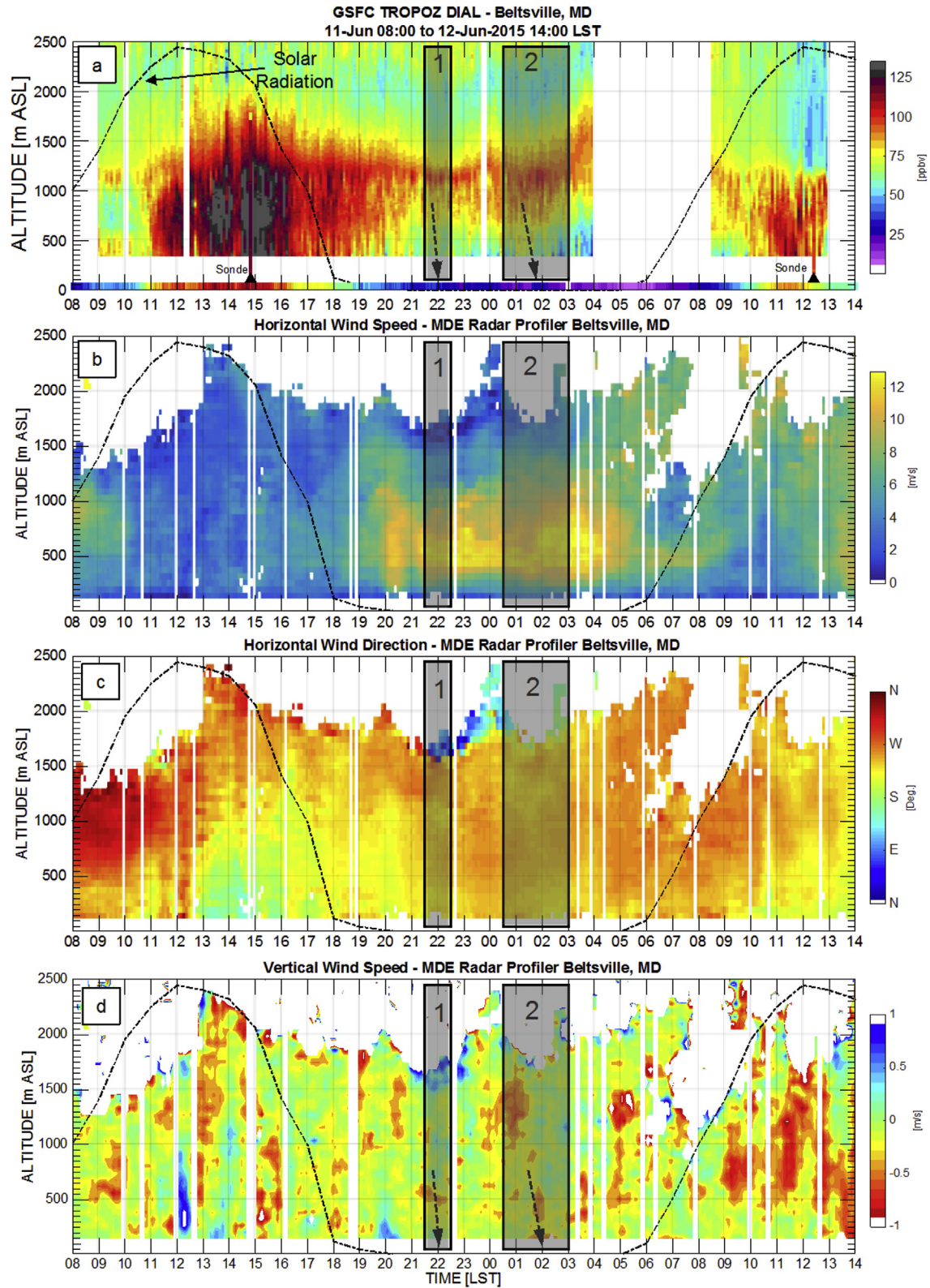
Fig. 4. (a) O₃ profiles from the GSFC TROPOZ DIAL at the Beltsville, MD site with two time segments. Two O₃ sondes are overlaid. The 1-min (Fig. 2) surface O₃ concentrations are in the bottom panel of the TROPOZ time series. The MDE Radar wind profiles are shown for b) horizontal wind speed, c) horizontal wind direction, and d) vertical wind speed. The solar radiation curve is also overlaid from the HU-Beltsville site to illustrate daytime/nighttime hours.
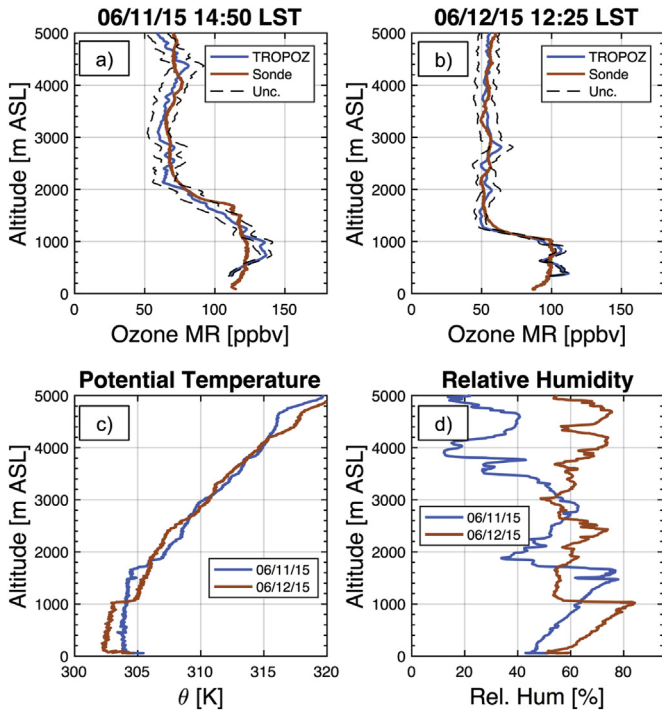
Fig. 5. Comparisons of the GSFC TROPOZ DIAL and the co-incident soundings for (a) 11 June 2015 at 14:50–14:56 LST and (b) 12 June 2015 at 12:25–12:31 LST. Potential temperature (c) and Relative humidity (d) soundings are also shown.

4. Regional simulations and observations

4.1. Meteorological simulations of the NLLJ

With the high "next-day" O_3 values (and one 70-ppbv NAAQS exceedance) sampled at downwind monitors in Maryland, it was imperative to isolate other potential downwind sites within the region that may have also been impacted by the NLLJ flow and entrainment of the polluted RL. Although these processes of

entrainment and increased O_3 are well characterized at the Beltsville, MD site, it was necessary to simulate the meteorological fields in order to accurately assess the contribution of the NLLJ transport in a regional context. A simulation was performed using the Weather Research and Forecasting (WRF) model. Initial and boundary conditions were derived from hourly Rapid Refresh (RAP) model data. WRF was configured with an outer domain and nest with ~350 × 350 horizontal grid points each, roughly centered over Beltsville, MD. The grid spacing was 4.5 km and 1.5 km for the outer domain and nest, respectively. The simulation was run with 80 vertical levels and the following physics: Mellor-Yamada-Janjic (MYJ) PBL parameterization [Janjic, 1994], four-layer Noah Land Surface Model, Morrison double-moment microphysics [Morrison et al., 2009], shortwave and longwave radiation with Rapid Radiative Transfer Model for GCMs (RRTMG) [Iacono et al., 2008], and Grell 3D cumulus parameterization [Grell and Dévényi, 2002] for the coarse domain only. The simulation began 07:00 LST on 11 June 2015 and continued for 36 h until 19:00 LST on 12 June. A comparison (Fig. S1) of the simulated wind speeds and the wind profiler observations at HU-Beltsville and Piney Run, MD (c.f. Fig. 1) are presented in the Supplemental.

The WRF wind fields during the onset of the NLLJ (21:00 LST on 11 June 2015) at the Beltsville site is shown in Fig. 7. The jet-like feature (designated within the dashed oval) has pronounced wind speeds in a mostly southerly/southwesterly flow. The jet extends from the western Carolinas, through the Mid-Atlantic region (and the HU-Beltsville lidar site), and into the southern New England region. There is a clear wind field gradient to the northward side of the jet that corresponds to an incoming cold front. The observations of O_3 and wind profiles in Fig. 4a reveal a decrease in O_3 to "cleaner" concentrations during the onset of the NLLJ. The concentrations below 1 000 m ASL were mainly between 50 and 60 ppbv, which resemble those in the free troposphere or from a region significantly less polluted. Fig. 6 indicates the jet air mass brought air from western Virginia/North Carolina area, which recorded MDA8 O_3 values of 55−65 ppbv. This corroborates the lidar analyses of transported "cleaner" air from this region to the Beltsville, MD site.

The WRF 4.5 km output was also utilized to calculate 21-h forward trajectories (Fig. 8 and time-height inset) initialized on 3 × 3 grids at three different levels above ground (AGL) near the Beltsville, MD site at 22:00 LST 11 June. A more detailed description of
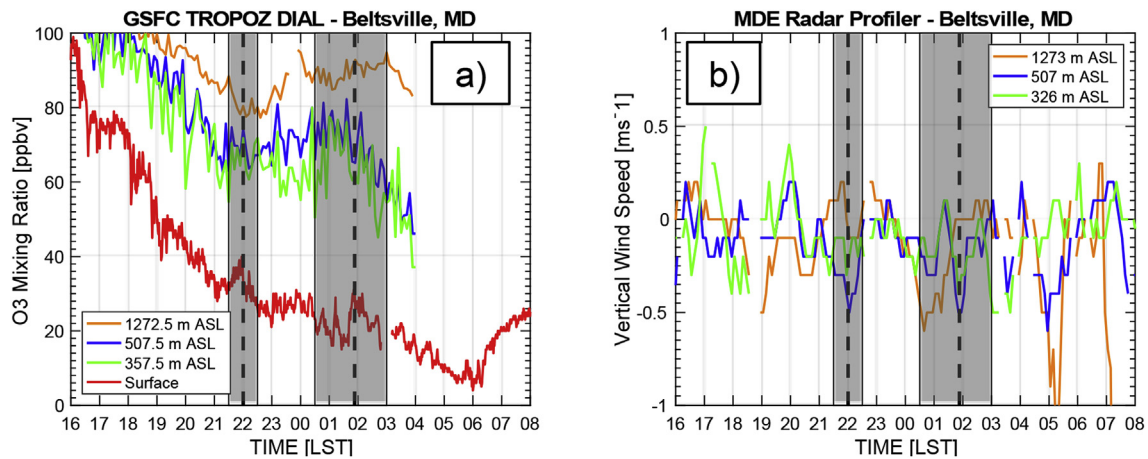

Fig. 6. Comparisons of O_3 derived from the TROPOZ lidar (a) and vertical wind speeds from the radar wind profiler (b) near 300, 500, and 1 200 m ASL. The surface ozone measurements are also overlaid in the first panel. The vertical dashed line indicates two regions with significant increases in surface ozone that are coupled with strongly descending air.
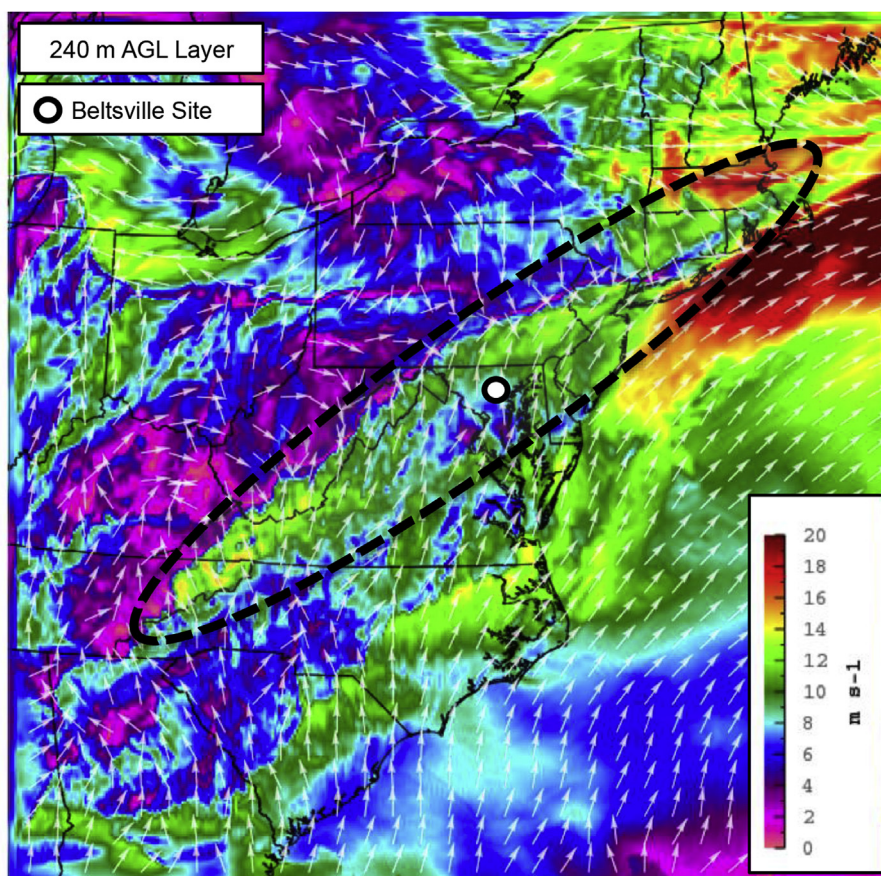
Fig. 7. WRF simulated wind field of the jet extending throughout the Mid-Atlantic region. The Beltsville site is denoted on the map.

the calculated trajectories is presented in the Supplemental. Trajectories were chosen at 200 m AGL (yellow), 400 m AGL (orange) and 1 000 m AGL (red) to represent the SL, air mass above the SL, and near the RL top, respectively as identified from the altitude and concentration from the O_3 lidar. All of the air mass trajectories are indicative of a generally northeasterly transport direction towards central New Jersey from the HU-Beltsville site. The yellow (SL) trajectories appear to mostly remain in New Jersey and are then transported northerly into the southern New England states or are transported out over the Atlantic Ocean. These trajectories remain mostly between 250 and 750 m AGL (Fig. 8b), indicating the surface pollutants were reasonably constrained within the SL during transport. The orange trajectories (above SL) are similarly advected, however several of these trajectory end points indicate the air mass at this level was transported over the Atlantic Ocean. Most of the red trajectories, representative of the RL mean flow, enter into the southern New England states, and are focused in the southern portion of the New England Region (New York (including Long Island), Connecticut, and Massachusetts).

A similar entrainment of the RL observed by the O_3 lidar near 09:00 LST is representative of the 1 000 m AGL trajectories. After 15:00 LST, most of the red trajectories quickly descend to altitudes between 500 and 1 500 m AGL. A sounding at Upton, NY and Chatham, MA (inset Fig. 8) at 19:00 LST on June 12 indicate a PBL height near 1800 and 2 500 m ASL, respectively, based on equivalent potential temperature. Thus, a majority of the trajectories that

were initialized in the polluted RL conditions at the HU-Beltsville site were transported overnight and well within the vertical region that would have been convectively mixed and entrained within the PBL on the following day at sites within the New England region.

4.2. "Next day" surface O_3 observations

In order to confirm the NLLJ-induced impacts of the chemical budget on the following day, 1-hr O_3 concentrations at 15:00 LST for 11 June and 12 June for the northeastern U.S (Fig. 9a–b) and inset view of southern New England states (Fig. 5c–d) are shown. The inset panels (Fig. 9c–d) were chosen based on the trajectory locations at 15:00 LST denoted by the WRF simulations (black 'x') and indicate monitoring sites that were located within the transport region of the RL and NLLJ.

On June 11, there were high O_3 levels across the eastern Great Lakes, Ohio River Valley, MA and southern New England regions (Fig. 9a). However the 12 June peak observations were mostly located in the New England region at coastal and inland locations (Fig. 9b). The monitoring sites that sampled higher O_3 concentrations are spatially correlated with the end trajectory path determined in the WRF trajectory. Similar to the trajectory points at 15:00 LST, centrally located high-O_3 regions occur in more inland locations such as northern New Jersey, central New York and western Connecticut and Massachusetts. Furthermore, three sites
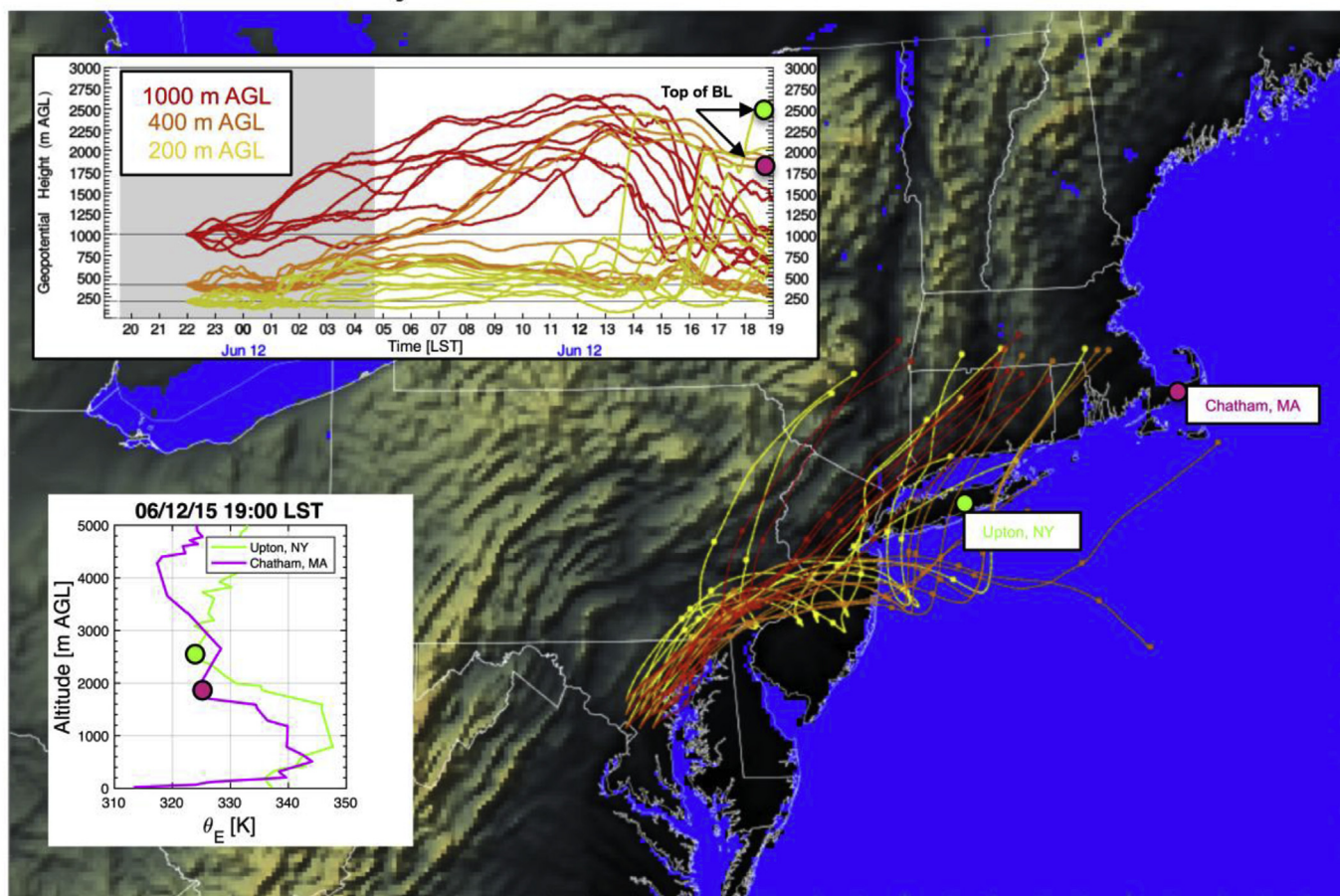
Fig. 8. Composite WRF forward trajectory was initialized in a 3 × 3 grid near the Beltsville, MD site at 22:00 LST on 11 June (segment 1 from Fig. 3) until 19:00 LST on 12 June using the 4 km wind fields at 200 m AGL (yellow), 400 m AGL (orange) and 1 000 m AGL (red). (For interpretation of the references to colour in this figure legend, the reader is referred to the web version of this article.)

on June 12 in Fig. 9d experienced MDA8 O_3 averages above the current 75 ppbv standard (Valley Central, NY, (84 ppbv), Ramapo, NY (81 ppbv), Danbury, CT (79 ppbv)) and additionally six more in the region would have exceeded the revised 70 ppbv standard (http://www.airnowtech.org). These exceedances, coupled with the lidar and sonde observations at the HU-Beltsville site exhibiting the direct entrainment of the RL into the PBL, confirm the high O_3 observed at sites in panel 9d were clearly impacted by NLLJ-induced regional transport.

5. Summary and conclusions

There are sparse records of continuous vertical profiles of O_3 within the United States and virtually none in nocturnal conditions except for dedicated campaign deployments. This lack of information has made it difficult to accurately evaluate nocturnal transport and "next day" entrainment of the polluted RL within a regional context. To better resolve these features, the GSFC TROPOZ DIAL was deployed to Beltsville, MD to take co-located measurements with the MDE radar wind profiler. These novel measurements have accurately identified the extent of O_3 concentrations and mixing heights during a high pollution event in the BW region. Following this, as the day-to-night transition occurred, the O_3 lidar continued observations and was able to accurately identify the concentrations

and height of a polluted RL during a NLLJ event and into the following morning. Downward transport of O_3 and its precursors during the jet event were also identified and reached the surface during two distinct segments at several sites throughout Maryland. Using meteorological simulations and a network of surface monitors, it was determined that the polluted conditions observed throughout the BW urban corridor were transported via the RL and NLLJ to the southern New England region and exacerbated "next-day" air quality. Specifically, this work has shown that the chemical budget in areas downwind of major urban centers can be altered significantly by events that occur overnight such as:

1. The development and depth of polluted residual layers (related to the onset of the NLLJ) occurring after poor air quality episodes and
2. Advection of the polluted residual layers over a regional scale; and on the following morning,
3. Entrainment of the polluted residual layer in the presence of the convectively growing boundary layer.

The authors recommend the union of a co-located ozone lidar and radar wind profiler, in conjunction with high-resolution modeling, as a more effective way to assess regional pollution transport. More observations are needed and will be critical to the
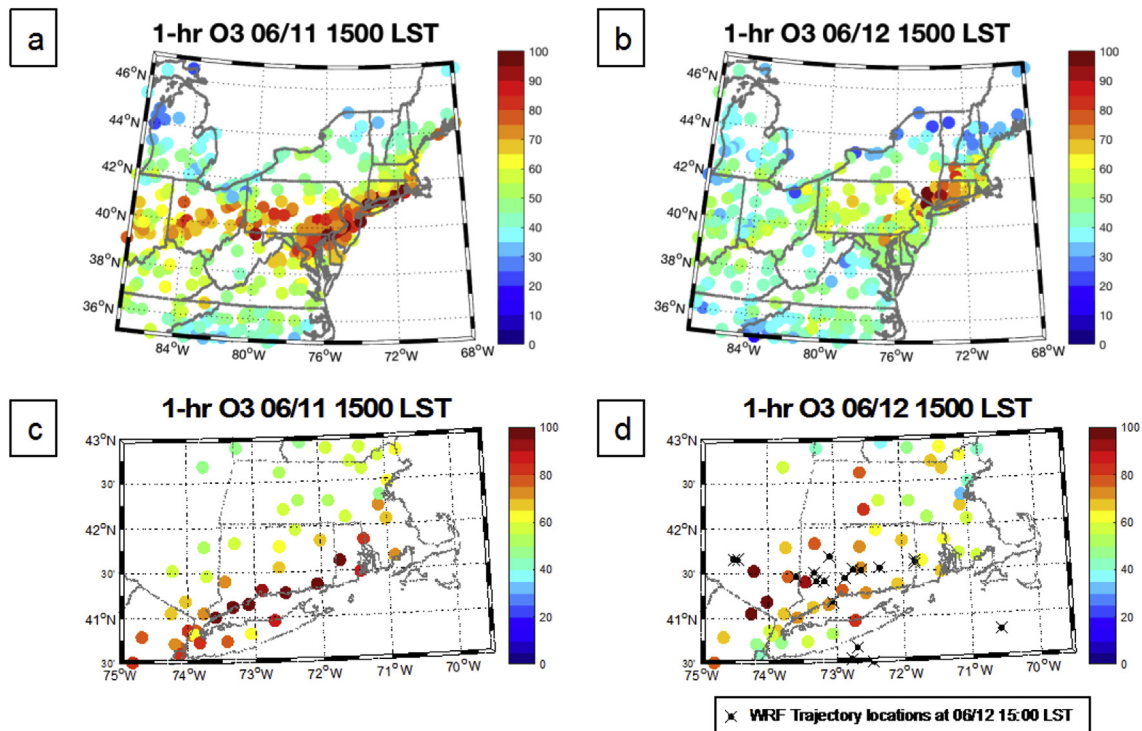
Fig. 9. The spatial distribution of 1-hr O$_3$ concentrations at 15:00 LST on 11 June and 12 June for the northeastern U.S. (a–b) and a subset of the region (c–d).

modeling community, where NBL pollutants above the surface have been historically difficult to verify. Ground based networks, such as the Tropospheric Ozone Lidar Network (TOLNet, http://www-air.larc.nasa.gov/missions/TOLNet/), are poised to answer these types of questions with deployable ozone lidars that have the ability to target complex urban regions with continuous profiling capabilities. However, a vast set of permanent O$_3$ lidar stations, situated throughout the northeastern U.S, would add to the confidence and understanding of overnight transport of O$_3$ in many complex urban settings. Particularly with the strengthening of the EPA regulations, it will be increasingly important to quantify and validate the nocturnal and early morning O$_3$ budget (aloft and at the surface) and assess the contribution of inter-state transport via mechanisms such as the NLLJ.

Acknowledgements

Appendix A. Supplementary data

Supplementary data related to this article can be found at http://dx.doi.org/10.1016/j.atmosenv.2017.03.039.

References

Ancellet, Gérard, Ravetta, François, 2005. Analysis and validation of ozone variability observed by lidar during the ESCOMPTE-2001 campaign. Atmos. Res. 74 (1), 435–459.

Aneja, Viney P., Mathur, Rohit, Arya, S.P., Li, Yongxian, Murray, George C., Manuszak, Thomas L., 2000. Coupling the vertical distribution of O$_3$ in the atmospheric boundary layer. Environ. Sci. Technol. 34 (11), 2324–2329.

Banta, Robert M., Senff, Christoph J., White, Allen B., Trainer, Michael, McNider, Richard T., Valente, Ralph J., Mayor, Shane D., et al., 1998. Daytime buildup and nighttime transport of urban O$_3$ in the boundary layer during a stagnation episode. J. Geophys. Res. Atmos. (1984–2012) 103 (D17), 22519–22544.

Banta, Robert M., Pichugina, Yelena L., Newsom, Rob K., 2003. Relationship between low-level jet properties and turbulence kinetic energy in the nocturnal stable boundary layer. J. Atmos. Sci. 60 (20), 2549–2555.

Banta, Robert M., Mahrt, Larry, Vickers, Dean, Sun, Jielun, Balsley, Ben B., Pichugina, Yelena L., Williams, Eric J., 2007. The very stable boundary layer on nights with weak low-level jets. J. Atmos. Sci. 64 (9), 3068–3090.

Beyrich, F., 1994. Sodar Observations of the Stable Boundary Layer Height in Relation to the Nocturnal Low-level Jet.

Compton, Jaime C., Delgado, Ruben, Berkoff, Timothy A., Hoff, Raymond M., 2013. Determination of planetary boundary layer height on short spatial and temporal scales: a demonstration of the covariance wavelet transform in ground-based wind profiler and lidar measurements*. J. Atmos. Ocean. Technol. 30 (7), 1566–1575.

Corsmeier, U., Kalthoff, N., Kolle, O., Kotzian, M., Fiedler, F., 1997. O$_3$ concentration jump in the stable nocturnal boundary layer during a LLJ-event. Atmos. Environ. 31 (13), 1977–1989.

Delgado, Ruben, Rabenhorst, Scott D., Demoz, Belay B., Hoff, Raymond M., 2014. Elastic lidar measurements of summer nocturnal low level jet events over Baltimore, Maryland. J. Atmos. Chem. 1–23.

Dreessen, Joel, John, Sullivan, Ruben, Delgado, 2016. Observations and impacts of transported canadian wildfire smoke on ozone and aerosol air quality in the Maryland region on June 9–12, 2015. J. Air & Waste Manag. Assoc. 66 (9), 842–862.

Drobinski, Philippe, Said, F., Ancellet, Gérard, Arteta, J., Augustin, P., Bastin, Sophie, Brut, A., et al., 2007. Regional transport and dilution during high-pollution episodes in southern France: summary of findings from the field experiment to constraint models of atmospheric pollution and emissions transport (ESCOMPTE). J. Geophys. Res. Atmos. 112 (D13).

EPA, 2015. Implementing the 2015 O$_3$ National Ambient Air Quality Standards. Accessed 1 December 2015. Available online at: http://www3.epa.gov/O3pollution/pdfs/20151001memo.pdf.

Grell, Georg A., Dévényi, Dezső, 2002. A generalized approach to parameterizing

convection combining ensemble and data assimilation techniques. Geophys. Res. Lett. 29 (14).

Hu, Xiao-Ming, Doughty, David C., Sanchez, Kevin J., Joseph, Everette, Fuentes, Jose D., 2012. Ozone variability in the atmospheric boundary layer in Maryland and its implications for vertical transport model. Atmos. Environ. 46, 354—364.

Hu, Xiao-Ming, Klein, Petra M., Xue, Ming, Zhang, Fuqing, Doughty, David C., Forkel, Renate, Joseph, Everette, Fuentes, Jose D., 2013. Impact of the vertical mixing induced by low-level jets on boundary layer O_3 concentration. Atmos. Environ. 70, 123—130.

Iacono, Michael J., Delamere, Jennifer S., Mlawer, Eli J., Shephard, Mark W., Clough, Shepard A., Collins, William D., 2008. Radiative forcing by long-lived greenhouse gases: calculations with the AER radiative transfer models. J. Geophys. Res. Atmos. 113 (D13).

Jacob, Daniel J., 2000. Heterogeneous chemistry and tropospheric O_3. Atmos. Environ. 34 (12), 2131—2159.

Jaffe, Daniel A., Wigder, Nicole L., 2012. Ozone production from wildfires: a critical review. Atmos. Environ. 51, 1—10.

Janjic, Zaviša I., 1994. The step-mountain eta coordinate model: further developments of the convection, viscous sublayer, and turbulence closure schemes. Mon. Weather Rev. 122 (5), 927—945.

Klein, Petra M., Hu, Xiao-Ming, Xue, Ming, 2014. Impacts of mixing processes in nocturnal atmospheric boundary layer on urban ozone concentrations. Bound. Layer Meteorol. 150 (1), 107—130.

Kuang, Shi, Newchurch, M.J., Burris, John, Wang, Lihua, Buckley, Patrick I., Johnson, Steve, Knupp, Kevin, Huang, Guanyu, Phillips, Dustin, Cantrell, Wesley, 2011. Nocturnal O_3 enhancement in the lower troposphere observed by lidar. Atmos. Environ. 45 (33), 6078—6084.

Maryland Department of the Environment, 2015. Ambient Air Monitoring Plan for Calendar Year 2016. http://www.mde.maryland.gov/programs/Air/AirQuality Monitoring/Documents/MDNetworkPlanCY2016.pdf.

McKendry, I.G., Steyn, D.G., Lundgren, J., Hoff, R.M., Strapp, W., Anlauf, K., Froude, F., Martin, J.B., Banta, R.M., Olivier, L.D., 1997. Elevated O_3 layers and vertical downmixing over the lower fraser valley, BC. Atmos. Environ. 31 (14), 2135—2146.

Morris, Gary A., Ford, Bonne, Rappenglück, Bernhard, Thompson, Anne M., Mefferd, Ashley, Ngan, Fong, Lefer, Barry, 2010. An evaluation of the interaction of morning residual layer and afternoon mixed layer O_3 in Houston using O_3sonde data. Atmos. Environ. 44 (33), 4024—4034.

Morrison, H., Thompson, G., Tatarskii, V., 2009. Impact of cloud microphysics on the development of trailing stratiform precipitation in a simulated squall line: comparison of one-and two-moment schemes. Mon. Weather Rev. 137 (3), 991—1007.

Poulos, Gregory S., Blumen, William, Fritts, David C., Lundquist, Julie K., 2002. CASES-99: a comprehensive investigation of the stable nocturnal boundary layer. Bull. Am. Meteorol. Soc. 83 (4), 555.Harvard.

Rabenhorst, S., Whiteman, D.N., Zhang, D.-L., Demoz, B., 2014. A case study of mid-Atlantic nocturnal boundary layer events during WAVES 2006. J. Appl. Meteorol. Climatol. 53 (11), 2627—2648.

Ryan, William F., 2004. The Low Level Jet in Maryland: Profiler Observations and Preliminary Climatology. Report for Maryland Department of the Environment, Air and Radiation Administration.

Ryan, William F., Doddridge, Bruce G., Dickerson, Russell R., Morales, Raymond M., Hallock, Kristen A., Roberts, Paul T., Blumenthal, Donald L., Anderson, Jerry A., Civerolo, Kevin L., 1998. Pollutant transport during a regional O_3 episode in the mid-Atlantic states. J. Air & Waste Manag. Assoc. 48 (9), 786—797.

Salmond, JrnA., McKendry, I.G., 2002. Secondary O_3 maxima in a very stable nocturnal boundary layer: observations from the Lower Fraser Valley, BC. Atmos. Environ. 36 (38), 5771—5782.

Seaman, Nelson L., Michelson, Sara A., 2000. Mesoscale meteorological structure of a high-O3 episode during the 1995 NARSTO-Northeast study. J. Appl. Meteorol. 39 (3), 384—398.

Stull, Roland B., 1988. An Introduction to Boundary Layer Meteorology, vol. 13. Springer Science & Business Media.

Sullivan, J.T., McGee, T.J., Sumnicht, G.K., Twigg, L.W., Hoff, R.M., 2014. A mobile differential absorption lidar to measure sub-hourly fluctuation of tropospheric O_3 profiles in the Baltimore—Washington, DC region. Atmos. Meas. Tech. 7 (10), 3529—3548.

Sullivan, John T., McGee, Thomas J., DeYoung, Russell, Twigg, Laurence W., Sumnicht, Grant K., Pliutau, Denis, Knepp, Travis, Carrion, William, 2015a. Results from the NASA GSFC and LaRC O_3 lidar intercomparison: New mobile tools for atmospheric research. J. Atmos. Ocean. Technol. 32 (10), 1779—1795.

Sullivan, John T., McGee, Thomas J., Thompson, Anne M., Bradley Pierce, R., Sumnicht, Grant K., Twigg, Laurence W., Eloranta, Edwin, Hoff, Raymond M., 2015b. Characterizing the lifetime and occurrence of stratospheric-tropospheric exchange events in the Rocky Mountain region using high-resolution ozone measurements. J. Geophys. Res. Atmos. 120 (24), 12410—12424.

Sullivan, J.T., et al., 2016. Quantifying the contribution of thermally driven recirculation to a high-ozone event along the Colorado Front Range using lidar. J. Geophys. Res. Atmos. 121 http://dx.doi.org/10.1002/2016JD025229.

Talbot, Robert, Mao, Huiting, Sive, Barkley, 2005. Diurnal characteristics of surface level O_3 and other important trace gases in New England. J. Geophys. Res. Atmos. 110 (D9).

Taubman, Brett F., Marufu, Lackson T., Piety, Charles A., Doddridge, Bruce G., Stehr, Jeffrey W., Dickerson, Russell R., 2004. Airborne characterization of the chemical, optical, and meteorological properties, and origins of a combined O3-haze episode over the eastern United States. J. Atmos. Sci. 61 (14), 1781—1793.

Thompson, Anne M., Witte, Jacquelyn C., GJ Smit, Herman, Oltmans, Samuel J., Johnson, Bryan J., WJH Kirchhoff, Volker, Schmidlin, Francis J., 2007. Southern Hemisphere Additional O_3sondes (SHADOZ) 1998—2004 tropical O_3 climatology: 3. Instrumentation, station-to-station variability, and evaluation with simulated flight profiles. J. Geophys. Res. Atmos. (1984—2012) 112 (D3).

Tong, Nelson YO, Leung, Dennis YC, Liu, Chun-Ho, 2011. A review on ozone evolution and its relationship with boundary layer characteristics in urban environments. Water, Air, & Soil Pollut. 214 (1—4), 13—36.

Trainer, M., Parrish, D.D., Buhr, M.P., Norton, R.B., Fehsenfeld, F.C., Anlauf, K.G., Bottenheim, J.W., et al., 1993. Correlation of O3 with NOy in photochemically aged air. J. Geophys. Res. Atmos. (1984—2012) 98 (D2), 2917—2925.

Tucker, Sara C., Banta, Robert M., Langford, Andrew O., Senff, Christoph J., Alan Brewer, W., Williams, Eric J., Lerner, Brian M., Osthoff, Hans D., Michael Hardesty, R., 2010. Relationships of coastal nocturnal boundary layer winds and turbulence to Houston O_3 concentrations during TexAQS 2006. J. Geophys. Res. Atmos. (1984—2012) 115 (D10).

Yorks, John E., Thompson, Anne M., Joseph, Everette, Miller, Sonya K., 2009. The variability of free tropospheric O_3 over Beltsville, Maryland (39N, 77W) in the summers 2004—2007. Atmos. Environ. 43 (11), 1827—1838.

Zhang, Jian, Rao, S. Trivikrama, 1999. The role of vertical mixing in the temporal evolution of ground-level O_3 concentrations. J. Appl. Meteorol. 38 (12), 1674—1691.

Zhang, Kesu, Mao, Huiting, Civerolo, Kevin, Berman, Stephen, Ku, Jia-Yeong, Rao, S. Trivikrama, Doddridge, Bruce, Philbrick, C. Russell, Clark, Richard, 2001. Numerical investigation of boundary-layer evolution and nocturnal low-level jets: local versus non-local PBL schemes. Environ. Fluid Mech. 1 (2), 171—208.

Zhang, Da-Lin, Zhang, Shunli, Weaver, Scott J., 2006. Low-level jets over the mid-Atlantic states: warm-season climatology and a case study. J. Appl. Meteorol. Climatol. 45 (1), 194—209.